

Coalescence of 3-phenyl-propynenitrile on Cu(111) into interlocking pinwheel chains

Miaomiao Luo,¹ Wenhao Lu,¹ Daeho Kim,¹ Eric Chu,¹ Jon Wyrick,¹ Connor Holzke,¹ Daniel Salib,¹ Kamelia D. Cohen,¹ Zhihai Cheng,¹ Dezheng Sun,¹ Yeming Zhu,¹ T. L. Einstein,² and Ludwig Bartels^{1,a)}

¹Pierce Hall, University of California-Riverside, Riverside, California 92521, USA

²Department of Physics, University of Maryland, College Park, Maryland 20742-4111, USA

(Received 9 June 2011; accepted 6 September 2011; published online 5 October 2011)

3-phenyl-propynenitrile (PPN) adsorbs on Cu(111) in a hexagonal network of molecular trimers formed through intermolecular interaction of the cyano group of one molecule with the aromatic ring of its neighbor. Heptamers of trimers coalesce into interlocking pinwheel-shaped structures that, by percolating across islands of the original trimer coverage, create the appearance of gear chains. Density functional theory aids in identifying substrate stress associated with the chemisorption of PPN's acetylene group as the cause of this transition. © 2011 American Institute of Physics. [doi:10.1063/1.3643715]

INTRODUCTION

The adsorption and subsequent self-assembly of molecules at metal surfaces provides a means of pattern formation on a length scale that has seen significant increases over the past decade;¹⁻³ originating at the sub-nanometer scale of individual small molecules,⁴ it now reaches all the way to the 10 nm scale, connecting (almost) seamlessly to the feature size accessible via e-beam lithographic techniques. In this quest for methods capable of patterning surfaces on an uninterrupted length scale, there is an obvious need to understand the role of intermolecular and substrate-mediated interactions in ordering adsorbate layers beyond the scale of their constituent molecules.⁵⁻⁸ In broad brush terms these intermolecular interactions can be intermolecular hydrogen bonds,^{6,9-11} metal coordination networks,¹²⁻¹⁶ or covalent bonds between adjacent species.¹⁷⁻²¹ Substrate-mediated interactions are most influential when they involve a surface state (e.g., on coinage metals) or elastic effects.²²⁻²⁷ In this paper, we show how a combination of hydrogen bonding and substrate-mediated interactions—tentatively attributed to surface stress—can generate arrays of interlocking pinwheels, each almost 5 nm across.

This work addresses 3-phenyl-propynenitrile (PPN) (see Fig. 1), a carbon-carbon triple-bond acetylene group carrying on one end a cyano group and on the other a benzene ring. Species without the nitrile group have been investigated by White's group;^{28,29} there the surface binding has been ascribed to interaction of the acetylene with the substrate via a double- σ bridge-bonded acetylene. Calculations involving only two substrate atoms suggested that the aromatic moiety points away from the substrate. In our theoretical work, we also find a global energy minimum for such a configuration; however, we additionally obtain a secondary minimum

for the aromatic ring and the cyano group close to the surface. This result corresponds much better with the scanning tunneling microscopy (STM) images and is, arguably, more intuitive since there is no obvious reason for the benzene ring to avoid interaction with the substrate charge density. A similar pattern has also been predicted by White's group absent of theoretical affirmation.²⁹ Given that both the experimental evidence from White's group on a closely related system and our own STM data both match the secondary minimum configuration, we take this to be the true binding geometry.

A number of papers reported on interactions between nitrile groups and adsorbed benzene rings, characterizing them as hydrogen bonding.^{9,10,15,30,31} While in the solution phase, hydrogen atoms attached to aromatic rings are insignificant hydrogen-bond donors,³² at the liquid nitrogen temperatures accessed in this study—and including the possibility for donation of charge density to the ring from the substrate—they have been found to determine patterns.^{5,11} In our proposed binding geometry the aromatic ring lies in a configuration which allows it to hydrogen bond to the nitrile group of a neighboring PPN molecule, suggesting that the patterns observed in this study are at least partially due to this effect. While hydrogen bonding does help account for the nearest neighbor interactions between PPN molecules, we will show that this interaction by itself cannot explain the observed pinwheel chains.

This paper focuses on the coexistence of two PPN patterns on Cu(111)—six-petal flowers and interlocking pinwheels, both at three molecules per 49 substrate atoms (resulting in a coverage of 6% of a monolayer)—and on the cause for the aggregation of seven flowers into a single pinwheel. The noteworthy seamless and commensurate coexistence of these phases will be thoroughly discussed. At higher coverage, a plethora of other structures were observed in which the molecules arrange more densely, in agreement with Sohn *et al.*'s results.^{28,29} Their multitude prevented us from understanding them in detail.

^{a)} Author to whom correspondence should be addressed. Electronic mail: Ludwig.Bartels@ucr.edu.

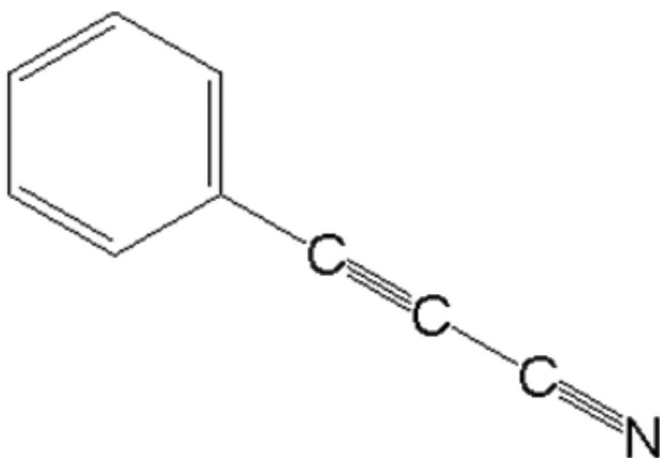


FIG. 1. Chemical structure of 3-phenyl-propynitrile (PPN).

EXPERIMENTAL AND COMPUTATIONAL SECTION

This paper describes a combination of STM imaging and density functional theory (DFT) modeling of molecular adsorption structures. All STM measurements proceeded on sputter-and-anneal cleaned samples of Cu(111), on which PPN was deposited at cryogenic temperatures (~ 100 K) followed by annealing to room temperature for ~ 1 h; prior to annealing no stable imaging conditions were achieved. The resultant low coverages leave roughly $2/3$ of the surface area unoccupied. PPN was obtained commercially from Aldrich.

Density functional theory calculations use the VASP code³³ with the PW92 generalized-gradient approximation³⁴ for the exchange-correlation functional and projected augmented waves. (For calculation of PPN adsorption geometries, the results were also verified with the plane-wave pseudopotential method³⁵ using ultrasoft pseudopotentials.³⁶) An electronic energy cutoff of 400 eV and augmentation charge cutoffs of 640–700 eV were used. We did not consider van der Waals (vdW) interactions since adsorption energy differences exceeded 1 eV; even if the adsorption energies were consequently underestimated, our main concern is with determining the geometry of the adsorption configuration. (Note that, e.g., while VASP calculations without vdW underestimate the 1/2 eV binding energy of benzene on Cu(111) and mangle the relative stability of unstable binding sites, they do find correctly that the most stable sites are nearly degenerate fcc and hcp hollows.³⁷ Furthermore, the standard vdW implementation in VASP has its own vagaries, e.g., incorrectly predicting a reconstruction of Ag(001).³⁸) Given the diffuse nature of vdW bonding, the effect on this aspect should be minimal. We also expect that inclusion of vdW will only enhance the relative stability of the flat conformation of PPN. All supercells use three substrate atomic layers of 6×4 copper atoms each, thus providing sufficient lateral space to prevent direct intermolecular interaction across the supercell boundary (i.e., >5 Å between any two atoms). A single \mathbf{k} point was used in each cell, with the exception of the data of Fig. 4(c), which uses $3 \times 3 \times 1$ \mathbf{k} points. All results are optimized so that the remaining forces are less than 0.04 eV/Å. We also performed temperature programmed

desorption (TPD) measurements, which agree with Sohn *et al.*'s data on phenylpropyne^{28,29} and are not shown here.

RESULTS

Figure 2 shows STM images of molecular islands of PPN on a Cu(111) surface exhibiting the coexistence between a pinwheel and a flower phase. The islands into which the molecules aggregate are surrounded by empty terrace area, indicating that attractive intermolecular (or substrate mediated) interactions are at play. All such islands are found attached to the lower side of copper step edges, suggesting that the latter serve as nucleation sites. Only some terraces contain molecular islands while others appear devoid of adsorbates, indicating that during room-temperature annealing, molecules are able to cross step edges. Individual molecules are mobile on Cu(111) even at liquid nitrogen temperatures; however, they are sufficiently slow to be observed during their diffusion to join molecular islands.

The molecular population of Fig. 2 consists of triplets of molecules forming a six-petal flower (Fig. 3(a)) and heptamers of such flowers whose peripheral molecules are rearranged to form interlocking pinwheels. We lightly colored flowers red and pinwheels green in Fig. 2(b) to facilitate their recognition. Approximately $2/3$ of all molecules are part of pinwheels. On many analyzed images, we barely ever find a flower-covered area between pinwheels that is sufficiently large to accommodate another pinwheel. Rather, the flower-covered areas appear to represent the interstitial space after coalescence of flowers into percolating pinwheel chains. The pinwheels interlock geometrically, thus forming “gear chains;” since each pinwheel owes its stability to the interplay between adsorbate-substrate and intermolecular interactions, these gear chains are not expected to be able to transmit rotation in any meaningful manner. The percolating nature of the pinwheels suggests that they formed sequentially; the presence of the flower phase in the interstitial area indicates that, once formed, the pinwheel chains are relatively rigid and stable.

Overlaying a grid on a portion of Fig. 2(b), we find that both the flowers and the pinwheels' teeth and cogs lie on a hexagonal lattice and in registry with each other. The flowers form a (7×7) $R23^\circ$ pattern, which may also be described as a $\begin{pmatrix} 8 & -3 \\ 3 & 5 \end{pmatrix}$ pattern; the pinwheels form a $(\sqrt{7} \times \sqrt{7})$ $R19^\circ$ superstructure of the flower pattern, which is a $(7^{3/2} \times 7^{3/2})$ $R3^\circ$ pattern or, in matrix notation, a $\begin{pmatrix} 19 & -1 \\ 1 & 18 \end{pmatrix}$ pattern. Its unit vectors are 47 Å long, its area is 1115 Å², and it contains 21 identical molecules. While complex patterns of identical molecules have been found in many adsorption systems, 21 molecules per unit cell rank among the most complex molecular patterns.^{5,10,16,39–41}

We performed DFT modeling of the adsorption of the molecule on a $6 \times 4 \times 3$ substrate atom supercell, determining the adsorption configuration shown in Fig. 3(d) (with adsorption energy ~ 0.84 eV). This configuration is in good agreement with Sohn *et al.*'s results for a substrate represented by two atoms only.²⁸ In ad-

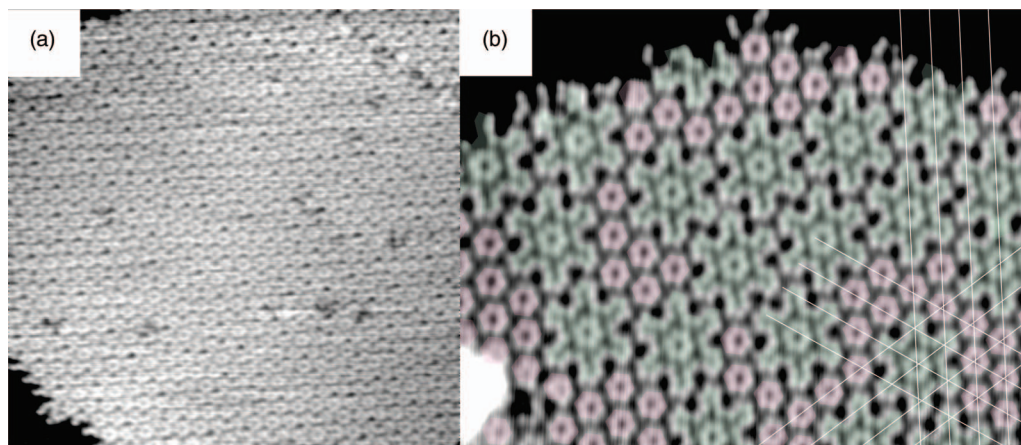


FIG. 2. (a) STM images of large islands of PPT on a Cu(111) terrace with a mixture of pinwheel and flower coverage. The top right corner shows a dislocation line in the island. (b) Enlarged view of the pinwheels (colored pale green) and flowers (colored pale red). High symmetry directions of the adlayer are indicated. Image parameters: (a) Bias: -1.3 V, current: 0.96 nA, image size: 42×41 nm² (b) Bias: -1.6 V, current: 80 pA, image size: 26×19 nm².

dition, we find—at substantially weaker adsorption energy (~ 0.41 eV)—a second adsorption configuration (minimized to forces < 20 meV/Å), in which both the ring system and the cyano group rest nearly flat on the substrate (Fig. 3(c)), in significantly better apparent agreement with the elongated shape of the molecular units in STM (see, for instances, the edges of the island in Fig. 2). In this configuration the cyano group and the benzene rings are nearly coplanar, which allows lateral interaction between the molecules, to be discussed in “Dis-

ussion” section. In both the cases, the molecule is primarily attached to the substrate by insertion of the carbon-carbon triple bond into a substrate bridge, in good agreement with Sohn *et al.*'s results.^{28,29}

DISCUSSION

In this section we propose an adsorption model for the flower and pinwheel structures, based on which we will explain the coalescence of the flower structures into pinwheels. These models rely on the adsorption configuration of PPN shown in Fig. 3(c), which is in much better geometric agreement with our STM images. In previous investigations of aromatic moieties pinned by reactive groups to metal surfaces,^{11,42–44} we generally found that the aromatic moiety comes to rest relatively close to the substrate, potentially providing some support for this configuration. While DFT codes quite consistently place aromatic species relatively far away from a metallic substrate,^{37,45–47} experimental evidence, such as from standing wave, x-ray absorption,⁴⁸ suggest a different behavior. Arguably, chemical intuition may also favor an adsorption configuration in which both the cyano and the phenyl group are sufficiently close to the substrate for interaction rather than pointing away from it, foregoing the opportunity of any interaction.

This adsorption configuration allows interpretation of the flower shapes as trimers of PPN molecules, in which the cyano nitrogen atom interacts with the hydrogen atom at the *meta* position of the phenyl ring (Fig. 3(a)). Such an interaction is in good agreement with, for instance, the interactions found in benzenethiol films.^{11,49} Aromatic hydrogen atoms have been found to form hydrogen bonds to nitriles and other nitrogen atoms in other organic groups quite frequently, further supporting our interpretation.^{9,10,15,30} The experimental resolution is insufficient to distinguish reliably between the cyano and the phenyl end of the molecule. Hence, it is unknown whether the film consists of trimers exclusively of one rotational orientation (enantiomer) or a (potentially ordered) racemic mixture of them.

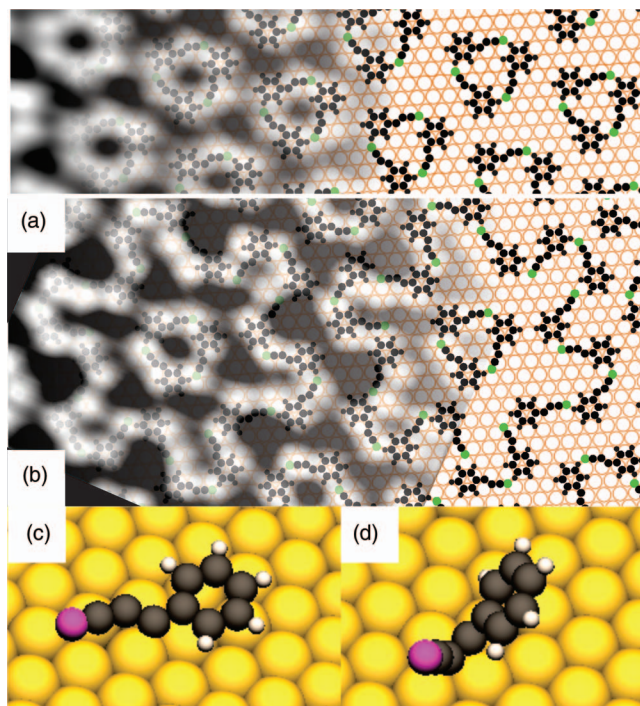


FIG. 3. (a) and (b) STM images of the flower and pinwheel phase and the corresponding models based on the adsorbate configuration shown in (c), which is a local minimum in our optimization. Panel (d) shows the PPN configuration on Cu(111) that has the highest binding energy according to our calculations. Image parameters: bias: -1.5 V, current: 0.12 nA.

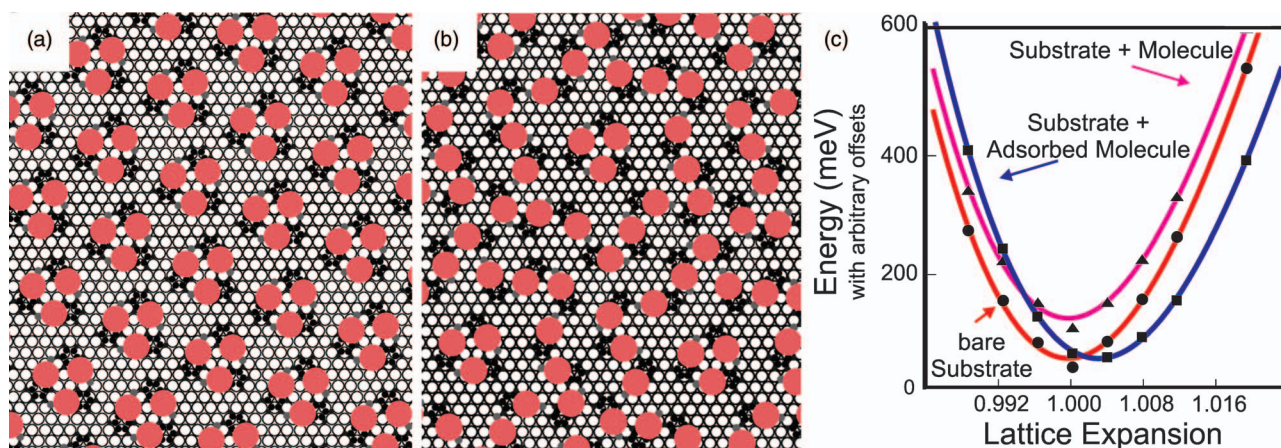


FIG. 4. Spatial distribution of the acetylene groups in (a) flower, and (b) the pinwheel structure. In the flower pattern the acetylene species are bunched more frequently in close trimers, although the overall coverage is identical to the pinwheel structure. Panel (c) shows the dependence of the total energy of a (circle) $6 \times 4 \times 3$ Cu slab, (triangle) Cu slab with a non-adsorbed acetylene molecule, and (squares) a Cu slab with an adsorbed acetylene molecule, on the copper lattice constant. The larger equilibrium energy indicates expansive stress induced by the di- σ interaction of PPN acetylene moiety with the substrate.

Starting out from this intermolecular interaction motif, we can construct a pinwheel structure that shows good agreement with the experimentally observed features (Fig. 3(b)). While the flower required only three rotational configurations of PPN on the substrate, the pinwheel requires six, as well as their inversion-symmetric counterparts. Thus, while in the flower shape all molecules adsorb at equivalent sites (due to the threefold symmetry of the substrate), for the pinwheel structure the molecule needs to be inverted, corresponding to a change between hcp and fcc hollow sites.

There is no readily apparent energetic benefit in the formation of the larger, more complicated and, hence, entropically disfavored pinwheel structure from the perspective of direct intermolecular interaction: if there were substantial energetic benefits from the slight variations between the intermolecular orientations in the pinwheel as compared to the flower pattern, a directly periodic arrangement of thus interacting species would be expected instead of the kind of coalescence of the flowers into larger superstructures observed here. Since the molecular patterns form on partially covered terraces, their molecular adlayer is not subjected to significant compressive stress or strain. Consequently, we look for a different origin of this phenomenon.

A close inspection of the primary interaction of PPN with the substrate suggests that the insertion of the acetylene group into a substrate atomic bridge creates expansive stress on the top substrate layer. Could this stress be the origin of the formation of the pinwheels? To substantiate this, Fig. 4 shows the flower and the pinwheel pattern, highlighting the locations at which the acetylene group inserts itself into a substrate atomic bridge: in the flower pattern, closely spaced triplets of this interaction are distributed on a regular hexagonal network. While at the center of a pinwheel the same triplet is found, the six peripheral locations in the pinwheel appear to distribute their 18 acetylene moieties more evenly (as opposed to clustering them in six triplets on a regular hexagonal grid). To evaluate this quantitatively, we calculated the spatial correlation between the acetylene moiety locations x in one pinwheel unit cell and the acetylene moiety locations in the

same unit cell as well as the six surrounding unit cells (i.e., a total of $(3 \times 7) \times 7(3 \times 7)$ acetylene moieties in pinwheel self and surrounding pinwheels $-(3 \times 7)$ self-correlation = 3066 distances r). We also calculated the same correlation for the flower pattern in the same area. Assuming, for simplicity, that the relaxation of the substrate stress is inversely proportional to the distance from the stress center (i.e., a $1/r$ potential), we find that the sum s over the reciprocal of all distances is about 0.4% smaller for the pinwheel structure than for the flower structure.

$$s = \sum_i^{\text{Acetylene moieties in center PW}} \sum_j^{\text{Acetylene moieties in seven PWs}} \frac{1}{|\vec{x}_i - \vec{x}_j|}$$

Clearly, a perfect $1/\text{distance}$ dependence of the stress potential is an oversimplification. However, a higher power would only increase the reduction of strain energy (e.g., a $1/r^2$ relationship leads to 2.4%), and a lower power (i.e., an even longer range potential) would be hard to justify.

Direct DFT modeling of these long-range interactions requires too large a supercell to be feasible. However, we can corroborate the presence of expansive stress caused by adsorption of an acetylene group on the substrate: to this end, we calculate the total energy of a $6 \times 4 \times 3$ substrate-atom supercell with no acetylene molecule attached, with an acetylene molecule in the vacuum above the substrate, and with the acetylene chemisorbed on the surface. We vary the geometric dimensions of the supercell to cause slightly larger or smaller lateral interatomic spacing of the copper atoms and relax all atoms in each case using $(3 \times 3 \times 1)$ \mathbf{k} -space mesh. For these calculations we maintain constant overall cell volume through variation of the amount of vacuum separating the slabs, in order to have constant net electron density in the unit cell to enhance comparability of the total energies obtained. Figure 4(c) shows the results: a quadratic fit of the total energy as a function of the lattice parameter shows a larger equilibrium unit cell for the case of acetylene substrate interaction than for the two cases without. This clearly

demonstrates that the kind of interaction found between PPN and the substrate exerts stress to expand the substrate lattice.

CONCLUSION

3-phenyl-propenenitrile (PPN) on Cu(111) forms a hexagonal network of molecular trimers, which coalesce into sequences (gear chains) of interlocking pinwheel-shaped heptamers. Density functional theory modeling of the adsorption of individual molecules results in two adsorption configurations, of which the one with the lower calculated binding energy appears to be the physically correct solution, representing a near-planar molecule in close proximity to the substrate. Evaluation of the lateral distribution of molecule-substrate interaction centers suggests relief of adsorption-induced surface strain as the driving force behind the formation of the large pinwheel structures.

ACKNOWLEDGMENTS

This work was supported by (U.S.) Department of Energy (DOE) grant (Grant No. DE-FG02-07ER15842) and by joint National Science Foundation (NSF) grant (Grant Nos. CHE 07-49949 (LB) and CHE 07-50334 (TLE)) with ancillary support from CNAM. Computational resources were made available by NERSC.

- ¹J. A. A. W. Elemans, S. B. Lei, and S. De Feyter, *Angew. Chem., Int. Ed. Engl.* **48**, 7298 (2009).
- ²L. Bartels, *Nat. Chem.* **2**, 87 (2010).
- ³J. V. Barth, *Surf. Sci.* **603**, 1533 (2009).
- ⁴G. A. Somorjai, *Introduction to Surface Chemistry and Catalysis* (Wiley, New York, 1994).
- ⁵G. Pawin, K. L. Wong, K. Y. Kwon, and L. Bartels, *Science* **313**, 961 (2006).
- ⁶J. A. Theobald, N. S. Oxtoby, M. A. Phillips, N. R. Champness, and P. H. Beton, *Nature (London)* **424**, 1029 (2003).
- ⁷U. Schlickum, R. Decker, F. Klappenberger, G. Zoppellaro, S. Klyatskaya, M. Ruben, I. Silanes, A. Arnau, K. Kern, H. Brune, and J. V. Barth, *Nano Lett.* **7**, 3813 (2007).
- ⁸D. Kuhne, F. Klappenberger, R. Decker, U. Schlickum, H. Brune, S. Klyatskaya, M. Ruben, and J. V. Barth, *J. Am. Chem. Soc.* **131**, 3881 (2009).
- ⁹T. Yokoyama, S. Yokoyama, T. Kamikado, Y. Okuno, and S. Mashiko, *Nature (London)* **413**, 619 (2001).
- ¹⁰U. Schlickum, R. Decker, F. Klappenberger, G. Zoppellaro, S. Klyatskaya, W. Auwärter, S. Neppel, K. Kern, H. Brune, M. Ruben, and J. V. Barth, *J. Am. Chem. Soc.* **130**, 11778 (2008).
- ¹¹K. Y. Kwon, G. Pawin, K. L. Wong, E. Peters, D. Kim, S. Hong, T. S. Rahman, M. Marsella, and L. Bartels, *J. Am. Chem. Soc.* **131**, 5540 (2009).
- ¹²U. Schlickum, R. Decker, F. Klappenberger, G. Zoppellaro, S. Klyatskaya, M. Ruben, I. Silanes, A. Arnau, K. Kern, H. Brune, and J. V. Barth, *Nano Lett.* **7**, 3813 (2007).
- ¹³N. Lin, A. Dmitriev, J. Weckesser, J. V. Barth, and K. Kern, *Angew. Chem. Int. Ed.* **41**, 4779 (2002).
- ¹⁴S. L. Tait, A. Langner, N. Lin, R. Chandrasekar, O. Fuhr, M. Ruben, and K. Kern, *ChemPhysChem* **9**, 2495 (2008).
- ¹⁵G. Pawin, K. L. Wong, D. Kim, D. Z. Sun, L. Bartels, S. Hong, T. S. Rahman, R. Carp, and M. Marsella, *Angew. Chem., Int. Ed. Engl.* **47**, 8442 (2008).
- ¹⁶P. Liljeroth, I. Swart, S. Paavilainen, J. Repp, and G. Meyer, *Nano Lett.* **10**, 2475 (2010).
- ¹⁷L. Grill, M. Dyer, L. Laffrentz, M. Persson, M. V. Peters, and S. Hecht, *Nat. Nanotechnol.* **2**, 687 (2007).
- ¹⁸J. A. Lipton-Duffin, O. Ivasenko, D. F. Perepichka, and F. Rosei, *Small* **5**, 592 (2009).
- ¹⁹M. Matena, T. Riehm, M. Stohr, T. A. Jung, and L. H. Gade, *Angew. Chem. Int. Ed.* **47**, 2414 (2008).
- ²⁰S. Hla, L. Bartels, G. Meyer, and K. Rieder, *Phys. Rev. Lett.* **85**, 2777 (2000).
- ²¹M. I. Veld, P. Iavicoli, S. Haq, D. B. Amabilino, and R. Raval, *Chem. Commun.* 1536 (2008).
- ²²E. C. H. Sykes, P. Han, S. A. Kandel, K. F. Kelly, G. S. McCarty, and P. S. Weiss, *Acc. Chem. Res.* **36**, 945 (2003).
- ²³N. Knorr, H. Brune, M. Epple, A. Hirstein, M. A. Schneider, and K. Kern, *Phys. Rev. B* **65**, 115420 (2002).
- ²⁴J. Repp, F. Moresco, G. Meyer, K. Rieder, P. Hyldgaard, and M. Persson, *Phys. Rev. Lett.* **85**, 2981 (2000).
- ²⁵F. Silly, M. Pivetta, M. Ternes, F. Patthey, J. P. Pelz, and W. D. Schneider, *Phys. Rev. Lett.* **92**, 016101 (2004).
- ²⁶Y. F. Wang, X. Ge, C. Manzano, J. Korger, R. Berndt, W. A. Hofer, H. Tang, and J. Cerda, *J. Am. Chem. Soc.* **131**, 10400 (2009).
- ²⁷M. Mehlhorn, V. Simic-Milosevic, S. Jaksch, P. Scheier, and K. Morgenstern, *Surf. Sci.* **604**, 1698 (2010).
- ²⁸Y. Sohn, W. Wei, and J. M. White, *Langmuir* **23**, 12185 (2007).
- ²⁹Y. Sohn, W. Wei, and J. M. White, *J. Phys. Chem. C* **111**, 5101 (2007).
- ³⁰D. Kuhne, F. Klappenberger, R. Decker, U. Schlickum, H. Brune, S. Klyatskaya, M. Ruben, and J. V. Barth, *J. Phys. Chem. C* **113**, 17851 (2009).
- ³¹S. Gao, J. Hahn, and W. Ho, *J. Chem. Phys.* **119**, 6232 (2003).
- ³²G. A. Jeffrey, *An Introduction to Hydrogen Bonding* (Oxford University Press, Oxford, UK, 1997).
- ³³G. Kresse and J. Hafner, *Phys. Rev. B* **47**, 558 (1993).
- ³⁴J. P. Perdew and Y. Wang, *Phys. Rev. B* **45**, 13244 (1992).
- ³⁵M. C. Payne, M. P. Teter, D. C. Allan, T. A. Arias, and J. D. Joannopoulos, *Rev. Mod. Phys.* **64**, 1045 (1992).
- ³⁶D. Vanderbilt, *Phys. Rev. B* **41**, 7892 (1990).
- ³⁷K. Berland, T. L. Einstein, and P. Hyldgaard, *Phys. Rev. B* **80**, 155431 (2009).
- ³⁸K. A. Fichthorn, H. Feng, and R. Sathiyarayanan, *Bull. Am. Phys. Soc.* **56**, March D31.08 (2011).
- ³⁹M. C. Blum, E. Cavar, M. Pivetta, F. Patthey, and W. D. Schneider, *Angew. Chem. Int. Ed.* **44**, 5334 (2005).
- ⁴⁰Y. C. Ye, W. Sun, Y. F. Wang, X. Shao, X. G. Xu, F. Cheng, J. L. Li, and K. Wu, *J. Phys. Chem. C* **111**, 10138 (2007).
- ⁴¹R. Coratger, B. Calmettes, M. Abel, and L. Porte, *Surf. Sci.* **605**, 831 (2011).
- ⁴²K. Y. Kwon, K. L. Wong, G. Pawin, L. Bartels, S. Stolbov, and T. S. Rahman, *Phys. Rev. Lett.* **95**, 166101 (2005).
- ⁴³Z. Cheng, E. S. Chu, D. Sun, D. Kim, Y. Zhu, M. Luo, G. Pawin, K. L. Wong, K.-Y. Kwon, R. Carp, M. Marsella, and L. Bartels, *J. Am. Chem. Soc.* **132**, 13578 (2010).
- ⁴⁴K. L. Wong, G. Pawin, K. Y. Kwon, X. Lin, T. Jiao, R. Fawcett, U. Solanki, L. Bartels, S. Stolbov, and T. S. Rahman, *Science* **315**, 1391 (2007).
- ⁴⁵D. Z. Sun, D. H. Kim, D. Le, O. Borck, K. Berland, K. Kim, W. H. Lu, Y. M. Zhu, M. M. Luo, J. Wyrick, Z. H. Cheng, T. L. Einstein, T. S. Rahman, P. Hyldgaard, and L. Bartels, *Phys. Rev. B* **82**, 201410 (2010).
- ⁴⁶A. Bilic, J. R. Reimers, N. S. Hush, R. C. Hofst, and M. J. Ford, *J. Chem. Theory Comput.* **2**, 1093 (2006).
- ⁴⁷M. Dion, H. Rydberg, E. Schröder, D. C. Langreth, and B. I. Lundqvist, *Phys. Rev. Lett.* **92**, 246401 (2004).
- ⁴⁸N. Koch, A. Gerlach, S. Duhm, H. Glowatzki, G. Heimel, A. Vollmer, Y. Sakamoto, T. Suzuki, J. Zegenhagen, J. P. Rabe, and F. Schreiber, *J. Am. Chem. Soc.* **130**, 7300 (2008).
- ⁴⁹K. Wong, K. Kwon, B. Rao, A. Liu, and L. Bartels, *J. Am. Chem. Soc.* **126**, 7762 (2004).